Hot Workability and Processing Maps

V.V.Kutumbarao[1] and T.Rajagopalachary[2]

[1]Department of Metallurgical Engineering, Banaras Hindu University,
Varanasi 221005

[2]Department of Metallurgical Engineering, Jawaharlal Nehru Technological University,
Hyderabad 500 872

1. Introduction

Hot working consists of mechanical processing of metals by techniques such as rolling, forging and extrusion at high homologous temperatures ($T > 0.5\ T_m$.). Obtaining a sound defect free product with close dimensional tolerances by a "Right the First Time" approach is becoming increasingly important in the hot working industry. Also net shape and near net shape technologies are becoming common. Mathematical modeling of hot working processes is a cost effective and speedy route to process optimization and process development. The entire process or only some specific aspect of it may be modeled.. Several models of varying complexity have been traditionally in use in hot working computations (Fig 1).

Recent developments in mathematical modeling of hot working have been taking place along three major directions. The first is the activity related to metal flow during hot working of components principally by the finite element method. Such models consider the workpiece as a continuum which is macroscopically homogeneous and has definite rheological properties. The second emerging direction is in the designing of manufacturing schedules which result in desired microstructures in a consistent fashion, such as in the controlled rolling of HSLA steels. Based on empirical relations for microscopic phenomena such as dynamic recovery, dynamic recrystallization, static recovery, static recrystallization and grain growth., this methodology, aims at calculation of microstructural parameters like grain size at each of several steps in the processing schedule. The third recent trend is to model the intrinsic hot workability of the material and to determine the optimum working conditions for processing in a single step. The dynamic materials model and the polar reciprocity model are two examples of this approach. These recent developments are discussed in the following sections.

2. Numerical and Phenomenological Models

2.1 Finite Element Analysis

Finite element analysis of flow simulation provides the forming engineer the information about time dependent fields such as velocity or displacement as also the stress tensor and the temperature. From the velocity or displacement fields the chnaging shape of the workpiece can be determined. From the stress field tensor the working load or torque can be determined. Several two and three dimensional finite element programs have been developed to model the metal flow in different forming processes. These programs differ from one another in the way the problem is mathematically formulated and its complexity, the rheological behaviour modeled, the way the friction is accounted for, the nature of the analysis attempted (transient or steady state), the reference frame with which the deformation and other tensors are characterized (Eulerian, Lagrangian, or an updated Lagrangian etc), the way thermomechanical coupling is modeled and the way the mesh is renewed (Gelten and Konter 1982, Huetnik et al 1988). Because of the large number of variables in metal flow simulation, the number of degrees of freedom rapidly becomes quite large for any three dimensional metal flow simulation. Due to this computational complexity, problem solving involving complex geometries of actual components has been somewhat limited. However flow simulations are expected to become more common as experience with various FEM codes increases, cost of   hardware dwindles and high performance graphics engines and more powerful algorithms become avaiable..

Finite element analysis usually assumes that the material is a homogeneous continuum so that the apparatus of continuum physics can be used. Changes in the internal structure are usually considered to reflect on the rheological behaviour. But the evolution of microstructure, as it occurs with increasing strain and number of forming steps, can not be predicted by the general formulations of the finite element method. A novel method of calculating the microstructure, which may be characterized by a parameter like the prior austenite grain size in steels, has been formulated by Sellars and coworkers. This is described in the next section.

2.2 Sellars Methodology

Many hot working schedules involve discrete strain steps interspersed with pause periods. The pause periods could range from a few hundredths of a second for rolling of wire rod to about one minute in flat rolling and forging operations. The deformation in a given step is usually small. Extrusion and plate rolling are the two exceptions where reductions greater than 80% in a single step are common. Microstructural changes occur due to microscopic phenomena such as dynamic recovery and dynamic recrystallization while the material is being strained and static recovery, static recrystallization, metadynamic recrystalization and grain growth during inter pass pauses. Thus the final structure obtained

in the hot worked component is a net result of its deformation history. Sellars and coworkers (e.g., Sellars and Whiteman 1979) have considered the different microscopic phenomena given above and provided algorithms for calculating the recrystallized fraction, grain size and grain boundary area. Starting with a reheated microstructure, change in the grain size produced as a result of recrystallization, recovery and grain growth following the first working step are computed. The updated value is used as the initial grain size for the second pass and so on in an iterative manner. The kinetics of each of the phenomena as a function of time and strain are followed independently and their influence on the microstructure and mechanical properties is calculated at every step. The kinetics of the phenomena depend on the initial microstructure and the processing conditions. A block diagram of the algorithm used by Sellars et al. (1980) is shown in Fig.2. The Inputs here are the initial grain size, the time -temperature profile, and the rolling parameters such as the rolling speed, diameter of rolls and the degree of reduction attempted. The algorithm makes use of empirical and phenomenological kinetic equations. The output consists of the specific grain boundary area, the retained strain and the grain size.

2.3 Hot Integrated Mathematical Simulation (HIMS)

A significant recent development is an integrated approach to metal forming which aims to bring in the work of several research workers under a common umbrella called HIMS. (Yoshida et al. 1991).

This simulation procedure can estimate simultaneously the temperature, the working force and torque, and the metallurgical properties from the exit of the reheating furnace to the finish of the final forming operation and subsequent cooling. This approach combines the finite element method of flow simulation in hot working with heat transfer analysis and the Sellars methodology described above. The metal forming system is considered to comprise of three simulators which are mutually coupled namely, the temperature simulator, the deformation resistance simulator and the metallurgy simulator. The deformation resistance simulator estimates parameters such as load, torque and motor power required for shape change, as well as the strain and stress distributions in the component. The temperature simulator estimates the temperature of the workpiece and the tooling. The metallurgy simulator estimates metallurgical properties like austenite grain size, the effect of phase transformations and the mechanical properties produced in the end product. This approach is useful in establishing an industrial working schedule for bulk production employing a given forming process. Like the other methods described above, the HIMS too does not consider the problem of defining and characterizing the intrinsic hot workability of the workpiece material.

3. Models Of Intrinsic Hot Workability

Intrinsic hot workability may be defined as the innate capacity of a material to undergo shape change during hot working. In the models defining the intrinsic hot workability, a macroscopic parameter is defined in such a way that it can be easily evaluated

from laboratory generated test data. The purpose is to determine the optimum working conditions of temperature and strain rate for hot working.

There are several microscopic phenomena which take place either simultaneously or in isolation in the deforming workpiece. These are dynamic recovery, dynamic recrystallization, dissolution and growth of particles, superplasticity, dynamic strain ageing, adiabatic shear banding, void formation at hard particles, wedge cracking at grain-boundary triple points, spheroidization of acicular and lamellar microstructures and reversal of strengthening mechanisms. Depending upon the nature of the material system and the processing conditions employed, different microscopic mechanisms may participate in the evolution of structure during working. The occurrence of any microscopic phenomenon usually has a bearing on the flow stress. The chosen intrinsic hot workabilty parameter should therefore be a sensitive function of the kinetics of the micromechanisms. The interpretation of processing maps based on the intrinsic workability parameter would be faciliated by the understanding of micromechanistic maps such as the Raj map described next.

3.1 Raj Micromechanistic Map

The Raj map is a plot in the strain rate and temperature space (Raj 1981). The map shows the boundaries delineating the occurrence of different microscopic phenomena in the deforming solid. These maps can be plotted to cover the warm and hot working temperature ranges of the material.. Construction of the map involves first the selection of probable microscopic phenomena. Appropriate equations are used to estimate the bounds of temperature and strain rates for these different micromechanisms. The areas enclosed by these bounds are the domains in which the particular microscopic phenomenon will prevail in metal deformation. The equations used to specify the bounds are obtained from suitable phenomenological models. The phenomena chosen by Raj for this purpose are dynamic recrystallization, adiabatic shear banding, wedge cracking at grain boundaries and cavity nucleation at hard second phase particles. Fig.3 shows a Raj processing map constructed for commercial purity titanium. The 'workability window' shown in Fig. 3 avoids the regions of undesirable phenomena like flow localization and fracture.

Elegant looking and easily interpreted, the Raj processing map is nevertheless purely micromechanistic. Validity of the model kinetic equations for complex alloys is uncertain. Further, in order to plot the map a variety of experimental data are required. Construction of the Raj processing map is possible only when considerable knowledge about the material is already available. The domains in the map are sensitive to the assumptions made regarding the microstructural features. For example, the cavitation domain boundary would depend sensitively on the assumed size and the spatial distribution of second phase particles(Fig 3).

While the Raj map no doubt serves a useful purpose, a really significant breakthrough in characterizing the intrinsic hot workability has occurred with the introduction of the dynamic materials model.

3.2. The Dynamic Materials Model

The dynamic materials model, propounded by Gegel and coworkers (Gegel 1988, Prasad et al. 1984) and popularized in India by Prasad and co-workers (1990), arose from considerations of physical systems modeling of Wellstead(1979). It finds its justification in the thermodynamic extremum principle enunciated by Ziegler (1963,1977). In formulating the philosophy of the model the proponents were seized of the question " how does a workpiece respond to the demands imposed on it by the hot working operation ? ". They postulated that the workpiece responds by exhibiting those processes which would maximize the rate of dissipation of energy. They visualized the metal working environment to be a system comprising three basic elements namely, the materials system, the control system and the equipment and tooling system respectively. The dynamic materials model is the connecting link between the material system and the control system. It considers the workpiece in hot working to be a nonlinear dissipator which dissipates energy as viscous heat and internal structural changes. This conceptualization allows one to treat the problem macroscopically, thereby avoiding the consideration of operative atomic processes (Gegel 1988).

In the dynamic materials model the total instantaneous power is split into two components G and J as in Eq. 1. The splitting is substantiated by a convex extremum principle known as the maximum rate of entropy production (Ziegler 1963).

$$\int dP = S\dot{E} = \int_0^{\dot{E}} S\, dE + \int_0^S \dot{E}\, dS \qquad (1)$$

where S and $\dot{E}$ are the instantaneous flow stress and strain rate respectively. The quantity G which is given by the area under the true stress - true strain rate diagram, is designated as "dissipator power content" and its complementary component J as the "dissipator power co-content". J in the model is assumed to be related to microstructural changes occurring concomitantly with the deformation while G is related to continuum effects.

From the convexity between a set of potential functions, according to the Ziegler' principle, it is possible to obtain the constitutive relation for a material system undergoing deformation as

$$S = C\dot{E}^m \qquad (2)$$

where C is a material constant and m is the strain rate sensitivity.

In the dynamic materials model, J is used to grade the hot workability of different materials. Since J is a function of strain rate and temperature, it is used to define the best operating conditions for hot working a given material by choosing a reference condition of the material.. An ideally viscous material obeys the constititive relation in Eq 2 with m=1. For this condition J =J$_{max}$. Hence it is possible to define a ratio

$$\eta = \frac{J}{J_{max}} = \frac{2m}{m+1} \tag{3}$$

The dimensionless parameter η is called as the "dissipation efficiency parameter" because it is considered to describe how well the workpiece dissipates power by microstructural changes relative to an ideal viscous condition. Optimum hot working conditions are deduced from the dissipation efficiency maps which show the variation of η in temperature and strain rate space.

For plotting η maps, true stress-true strain data are determined from uniaxial tension or compression or torsion tests at several combinations of temperature and strain rate.. From these flow stress values the dissipation efficiency maps are plotted by numerical differentiation. and interpolation. Gegel (1988, Zhao *et al*. 1992) and Prasad and coworkers (e.g. Padmavardhani and Prasad 1992) have constructed the dissipation efficiency maps for a number of metals and alloys, including Ti-6242, nimonic alloys, titanium and nickel aluminides, copper alloys, aluminum and its alloys, nickel and its alloys, stainless steels, zirconium alloys and several other materials. Peaks and valleys in these maps may be associated with certain microstructural changes. A representative example of these maps is shown in Fig. 4 for an ($\alpha+\beta$) titanium alloy Ti-6Al-2V-4Mo-2Cr. This map shows a peak around 925°C and 10^{-1}s^{-1} which is associated with the occurrence of dynamic recrystallization of the α phase.

Different microscopic phenomena have different dissipation efficiencies and other characteristic features which help in their identification in the map. Phenomena which are beneficial to hot workability such as dynamic recovery and dynamic recrystallization display high dissipation efficiencies.However, since phenomena detrimental to hot workability such as cracking and void formation also possess high dissipation efficiencies, a means of separating them from the former is required in order to use the dissipation efficiency maps for optimizing the hot working conditions. For this purpose regions in the map associated with instabilities are identified with the help of suitable stability criteria.(Malas 1985, Kumar 1987, Gegel 1988). Only after superimposition of the inastability map dissipation defficiency map be considered a processing map.

The strength of the dynamic materials model is that it captures the most important characteristic of the deforming workpiece in hot working namely, the strain rate dependance of the flow stress. Because of this fact a correlation between the topographic features in the η map and the microscopic phenomena in the corresponding Raj map is normally found. The effect of strain history on the hot working schedule has not been considered to be

significant In the dynamic materials model. Memory or deformation history dependence is a basic feature of metallic materials exhibiting rate dependent and rate insensitive flow behaviour. At hot working temperatures, the history dependence may be small but cannot be neglected altogether (Alexander 1989).

3.3 Polar Reciprocity Model

This model has been introduced to provide for the deformation history dependence of flow stress while at the same time recognizing the strong strain rate dependence of flow stress as the primary flow characteristic of the workpiece.(Rajagopalachary and Kutumbarao 1989).

For defining the intrinsic hot workability parameter, thie model involves the normality principle of classical theory of plasticity. A polar reciprocity relation between two first degree nonlinear potential functions in stress and strain rate spaces respectively is used (Fig.5). From this relation it is possible to partition the total instantaneous power of inelastic deformation into two components. The flow stress-strain rate curve is the boundary separating the two split components. From the normality principle it follows that the flow stress-strain rate relation is a power law. Hill (1987) has constructed first degree homogeneous dual potential surfaces and established their one to one relation . Fig. 6. shows a convex potential surface $\Phi = K$ in stress space with origin O_1. Let an arbitrary radius vector O_1P at point P on Φ be given. The magnitude of the normal to Φ at P is scaled so that it is equal to KK'/Φ where KK' is equal to the power being expended. For every point P on Φ a corresponding point P' on Φ' may be found by drawing a parallel vector from O_1 in the direction ν with a scaled normal as above. The points p' on Φ' then define a potential surface in strain rate space. The terms K and K' are scalar valued functions of temperature and deformation history. The two conjugate potential functions can be dependent on variables which may not be subject to the polar reciprocity relation. The effect of strain or deformation history is taken into account with such variables. With this background, the model considers the rheology of the material to be viscoplastic flow of the form ;

$$S = H(E^P) + c\,G(\dot{E}^P) \qquad\qquad (4)$$

where $H(E^P)$ and $G(\dot{E}^P)$ denote respectively the history dependent and strain rate dependent functions of flow stress S and c is a constant. One of the split power components is used to define the model parameter ζ for the intrinsic hot workability as

$$\zeta = 1 - \left(\frac{S - H(E^P)}{S}\right)\left(\frac{2m'}{(2m'+1)}\right) \qquad\qquad (5)$$

in which m' is the modified strain rate sensitivity.

Tests such as uniaxial compression or plane strain compression at several hot working strain rates and temperatures are adequate for the evaluation of ζ. The chosen temperature and strain rate levels form a grid of points in temperature and strain rate space. A ζ map can be constructed at a strain E_1 as follows. From the stress-strain diagram the flow stress at E_1 is known. The area under the flow curve upto E_1 can be determined by numerical quadrature. The minimum in flow curve upto E_1 is determined. The product $S_{min} E_1$ is subtracted from the above area. This difference is normalized by the area under the flow curve upto strain E_1. This fraction is equal to the fraction of the history dependent component of flow stress (S_b/S) which is the history dependent component of flow stress. This is by constitutive assumption. This procedure is repeated for grid points in temperature-strain rate space.. The strain rate dependent components are determined from Eq. 4.. Grid point values of the rate dependent components of flow stress are utilized to evaluate the modified strain rate sensitivity of the material m'.. Knowing the modified strain rate sensitivity, the flow stress and the history dependent component of flow stress at any grid point, it is possible to evaluate zeta.. The ζ values at the grid points are used to obtain two dimensional contour and three dimensional surface maps in strain rate and temperature space. Several such maps can be plotted for a given material at different plastic strain levels.

The ζ maps exhibit different topographic features.(Fig.7). An elaborate exercise has been carried out by Rajagopalachary(1994) to establish a correspondence between the topographic features in the ζ maps of titanium alloys and the microscopic phenomena that take place concurrently with shape change. This exercise included a close examination of post deformation microstructures and the phenomenological characteristics of deformation. Some of the important conclusions that emerge from this study are: (a) Phenomena involving creation,rotation and migration of interfaces result in ζ basins in the maps. This is the case with phenomena like superplasticity, spheroidization of lamellar phases and dynamic recrystallization. The ζ-basins are considered to be repositories of good hot workability. (b) Grain growth would cause large increase in ζ and poor intrinsic hot workability. Flow localization that leads to adiabatic shear banding and fracture would also produce high ζ hills or plateaus. A correspondence between the magnitude of ζ and the microscopic phenomena that were observed is given in Table.1.

Many microscopic phenomena are known to possess a characteristic strain threshold for initiation. The characteristic strain threshold as also the kinetics of the phenomena may be functions of strain rate and temperature. Such functional dependency produces motion of the domains in the ζ maps with plastic strain. This may be illustrated by the behaviour exhibited by $(\alpha + \beta)$ titanium alloy BT9 (Fig.8) This alloy exhibits a microscopic phenomenon called "grain pinching" over a temperature range 900 - 970^{0}C and strain rate range 10^{-3} to 10^2 s^{-1}. This is a structure homogeneization process in which the interface between the α and β phases breaks down. The local protrusions or necks "pinch" (that is consume) the other phase progressively, to produce an equiaxed and refined grain

structure. In this process a large interface area is created. Corresponding to this process a ζ basin is seen in the processing map of the alloy. This domain would shift from a high temperature to a low temperature as strain is increased. Such observations have the implications that, (a) zeta could vary sensitively with the plastic strain and (b) while predicting the optimum conditions of hot working from the zeta maps, the magnitude of plastic strain in the component should also be considered.

Fig.9 shows the domains of prevalence of some microscopic phenomena in a range of titanium alloys identified on the basis of the corresponding ζ maps. A good agreement has been found between the optimum working conditions predicted by the polar reciprocity model and the actual industrial working schedules for the alloys studied. This is evident from Table 4. An important feature of the processing maps based on the polar reciprocity model is that microscopic phenomena which promote good workability occupy regions that are sufficiently distinct from those occupied by phenomena which are detrimental to workability. For example flow localization and fracture are always associated with high zeta hills or plateaus, while dynamic recrystallization and superplasticity are associated with ζ basins or valleys. Hence the superimposition of a stability condition to separate the two processes is not necessary. A zeta value approaching 1 is definitely a condition of instability.

4. Conclusions

The recent developments in mathematical modeling strive to satisfy the increasingly exacting demands of the forming engineer charged with producing sound components at minimum cost. Simulation of metal flow during hot working has been attempted. Integrated simulations where coupling between metal flow, heat transfer and phase change are well formulated are at a nascent stage. The algorithms for calculating microstructural parameters are reasonably well established.. Such calculations may become routine in determining the optimum deformation sequence in rolling mills. They need to be evaluated for other hot working processes as well. Intrinsic hot workability studies are likely to become an integral part of material development and characterization programmes., Interesting results may be expected to emerge when the three listed directions of mathematical modeling can be combined into a unified approach.
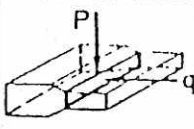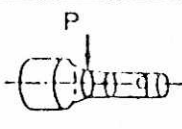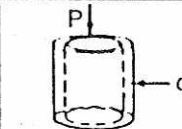
References

Alexander J M ,1989, In Modeling of Hot Deformation of Steels, J G Lenard (ed), Springer-verlag, Belin, p 101

Gegel H L , 1988, Metals Handbook, Vol 14, Forming and Forging, p 407

Hill R , 1987, Journal of Mechanics and Physics of Solids, Vol 35 , p23

Huetink J , Van Del Lugt and Vreede T , 1988, In Modelling of Metal Forming Processes, J L Chenot and E Onate (eds), Kluwer.

Kumar A K S,' Criteria for Predicting Metallurgical Instabilities in Processing', M.S. Thesis, I.I.Sc, Bangalore, Oct.1987.

Malas J C , A Thermodynamic and Continuum Approach to the Design and Control of Precision Forging Processes, M.S.Thesis, Wright State University, Dayton, Ohio, 1985.

Padmavardhani D and Prasad Y V R K , 1992, Materials Science and Engineering, A155.

Prasad Y V R K, Gegel H L , Doraivelu S M , Malas J C, Morgan J T , Lark K A and Barker D R , 1984, Metallurgical Transactions., Vol 11A, p 1883.

Prasad Y V R K,1990, Indian Journal of Technology, Vol 128, p 435

Raj R ,1981, Metallurgical Transactions , Vol 12A, p 1089

Rajagopalachary T and Kutumbarao, 1989, Metals, Materials and Processes, Vol 1, p57

Rajagopalachary T , Ph D Thesis, Banaras Hindu University, Varanasi, INDIA, 1994

Sellars C M , 1980, Sheffield International Conference on Hot Working and Forming Processes, C M Sellars and G J Davies (eds), Met. Soc., England, p3.

Wellstead P E ,1979, In Introduction to Physical Systems Modelling, Academic Press, London,

Yue S and Jonas J J , 1990, Materials Forum, Vol14, p 245.

Zeigler H , Progress in Solid mechanics, Vol 4, John Wiley, N.Y., 1963, p 93-193.

Zeigler H , 1977, An Introduction to Thermodynamics, North-Holland Publ.Co.

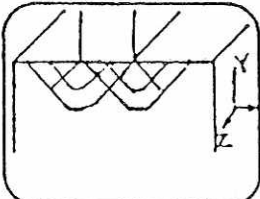Zhao D , Tuler I R and Lloyd, 1992, Scripta Meallurgica et. Materialia, Vol 27, p 41

MATHEMATICAL MODELLING

A Set of Fundamentally based Differential Equations which Provide Quantitative Description of The Metal Forming Process.
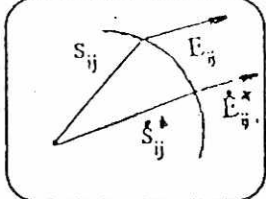
(a) SLAB METHOD

Assumptions : 1. Homogeneous deformation 2. Stress or strain gradient In one direction only	slab model P q	slices model P	tube model P q	•Approximate Strain or Load in the component

(b) SLIP LINE FIELD METHOD

Assumptions :
. Rigid-Plastic
  Flow Behaviour

Limitations :
•Provides load
  Estimate only

•Tedious, Solutions
  Difficult to verify

(c) UPPER BOUND METHOD

Based on limit theorem :
Power Dissipated Actually
< power expended in a
kinematically admissible
Velocity field

S_{ij} $\dot{E}_{ij}$
$\dot{E}_{ij}^{x}$
$\dot{S}_{ij}$

•Provides an estimate
of load and power
involved in forming a
component

(d) LOWER BOUND METHOD

Based on limit theorem :
Power actually dissipated > power expended by
a statically admissible stress field

Provides estimate of minimum power and load in
forming a component

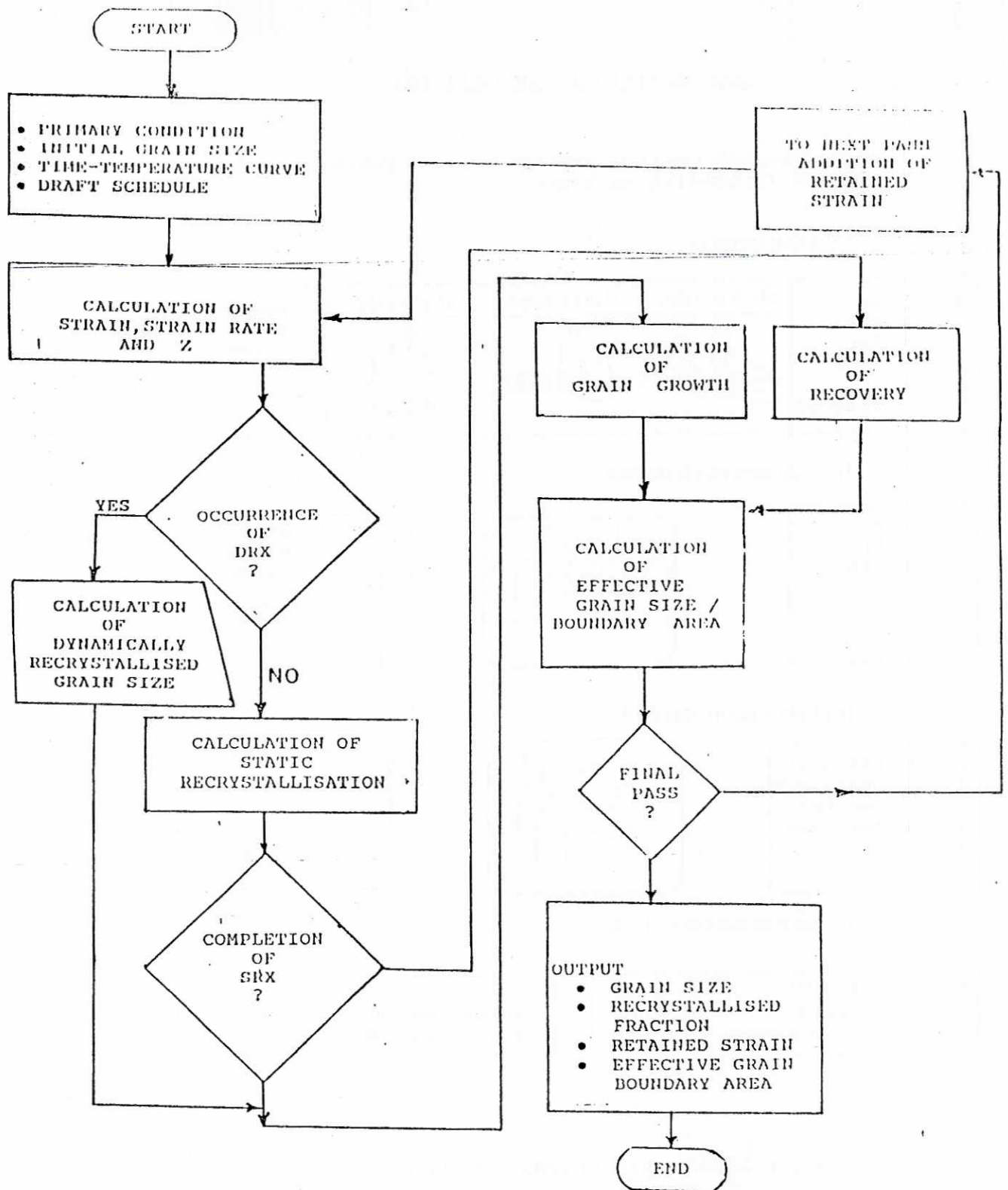Fig 1. Mathematical Models in Metal Processing.

Fig 2. Block Diagram Illustrating the Algorithm Used in the Metallurgy Simulator

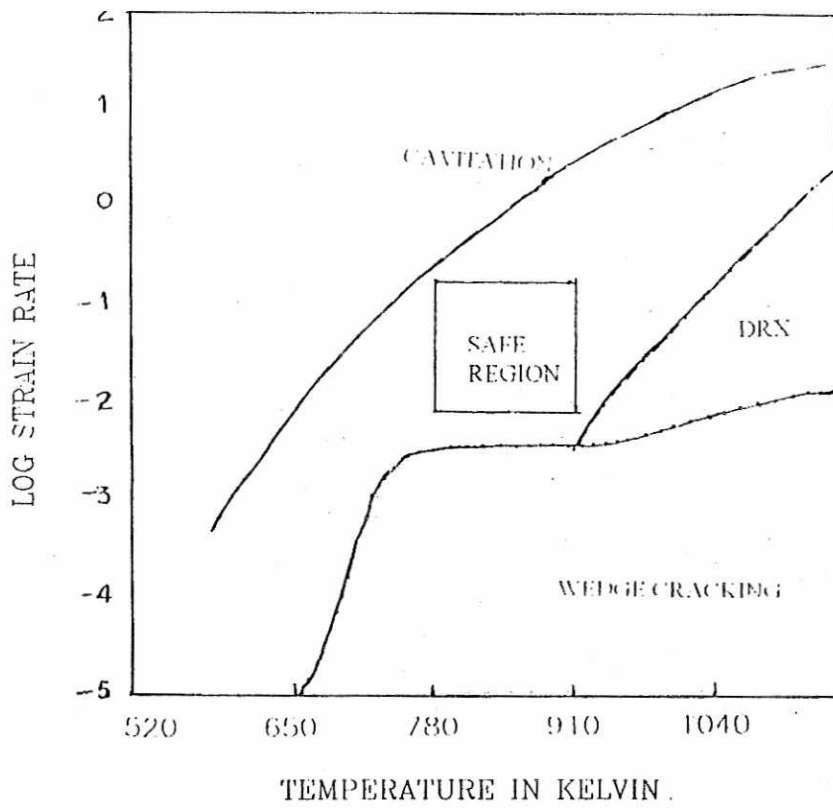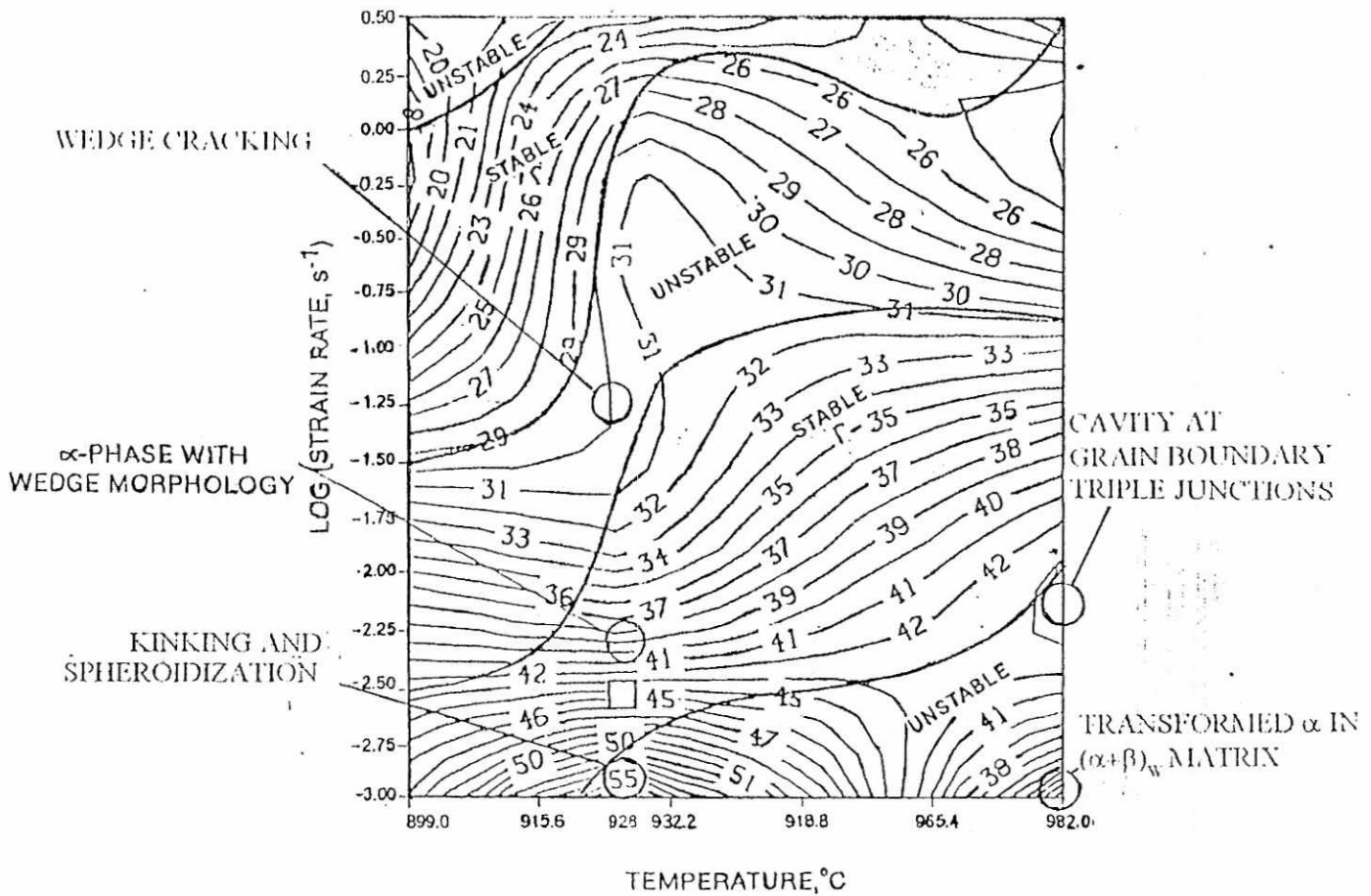*Fig* 3. Raj type Micro-Mechanistic Processing Map for Commercial Purity Titanium.

Fig 4. The Dissipation Efficiency Map for Ti 6242 Alloy. **(Gegel ,1988)**
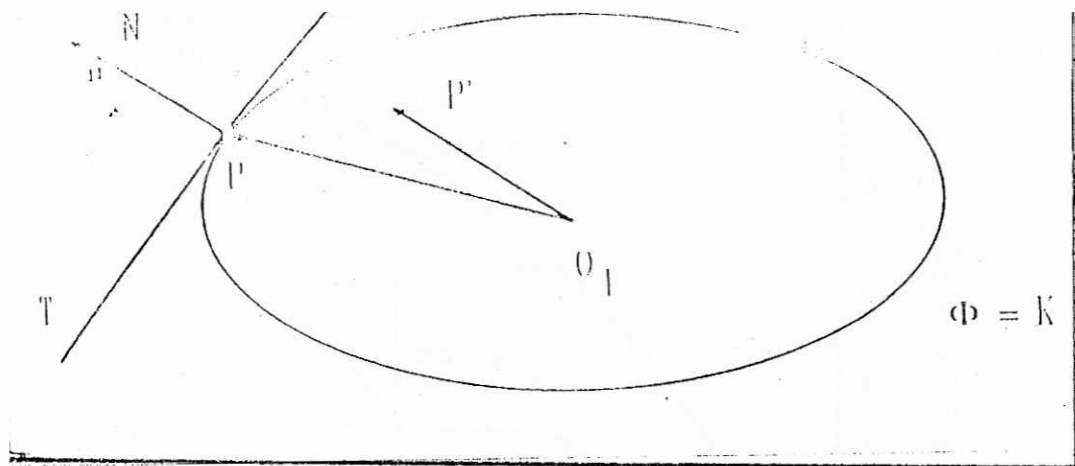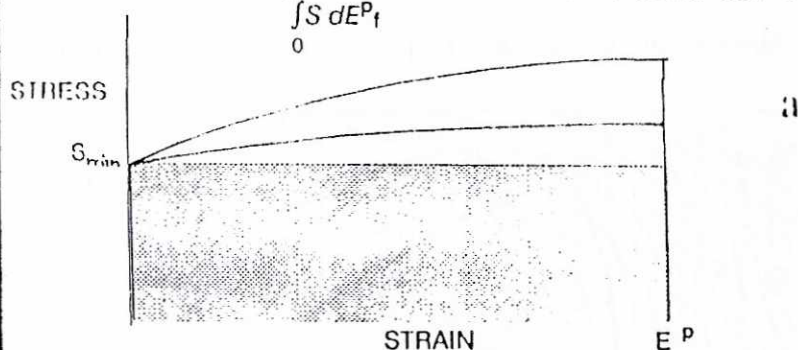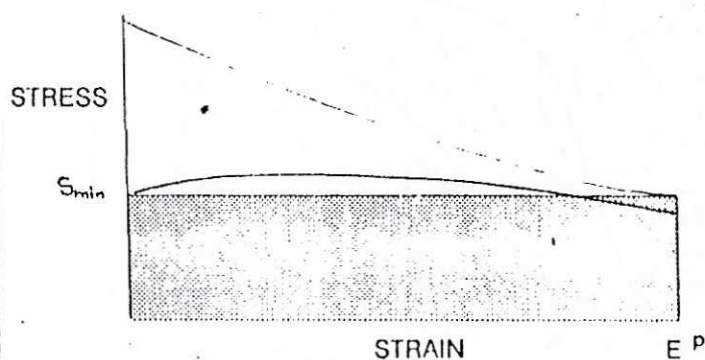
Fig 5. Pole-Polar Relationship Between two Convex Potential Funtions In Stress and Strain Rate Spaces.

H (E^P) is obtained from the true stress-true strain curves

$$\frac{H(E^P)}{S} = \frac{\int_0^{E^P} S\, dE^P_f - \int_0^{E^P} S_{min}\, dE^P_f}{\int_0^{E^P} S\, dE^P_f} = \frac{Area\ above\ S_{min}\ Horizontal}{Area\ below\ flow\ curve}$$

Case 1 : Work hardening Behaviour :   H(E^P) increases with strain

Case 2 : Flow softening   : H(E^P) Decreases and levels off

Case 3 : Ideal plastic behaviour : H(E^P) = 0

Fig 6. **Choice of History Function and its Behaviour Under Different Conditions of Plastic Flow**

ZETA CONTOUR PLOT FOR CP TITANIUM   0.1 STRAIN
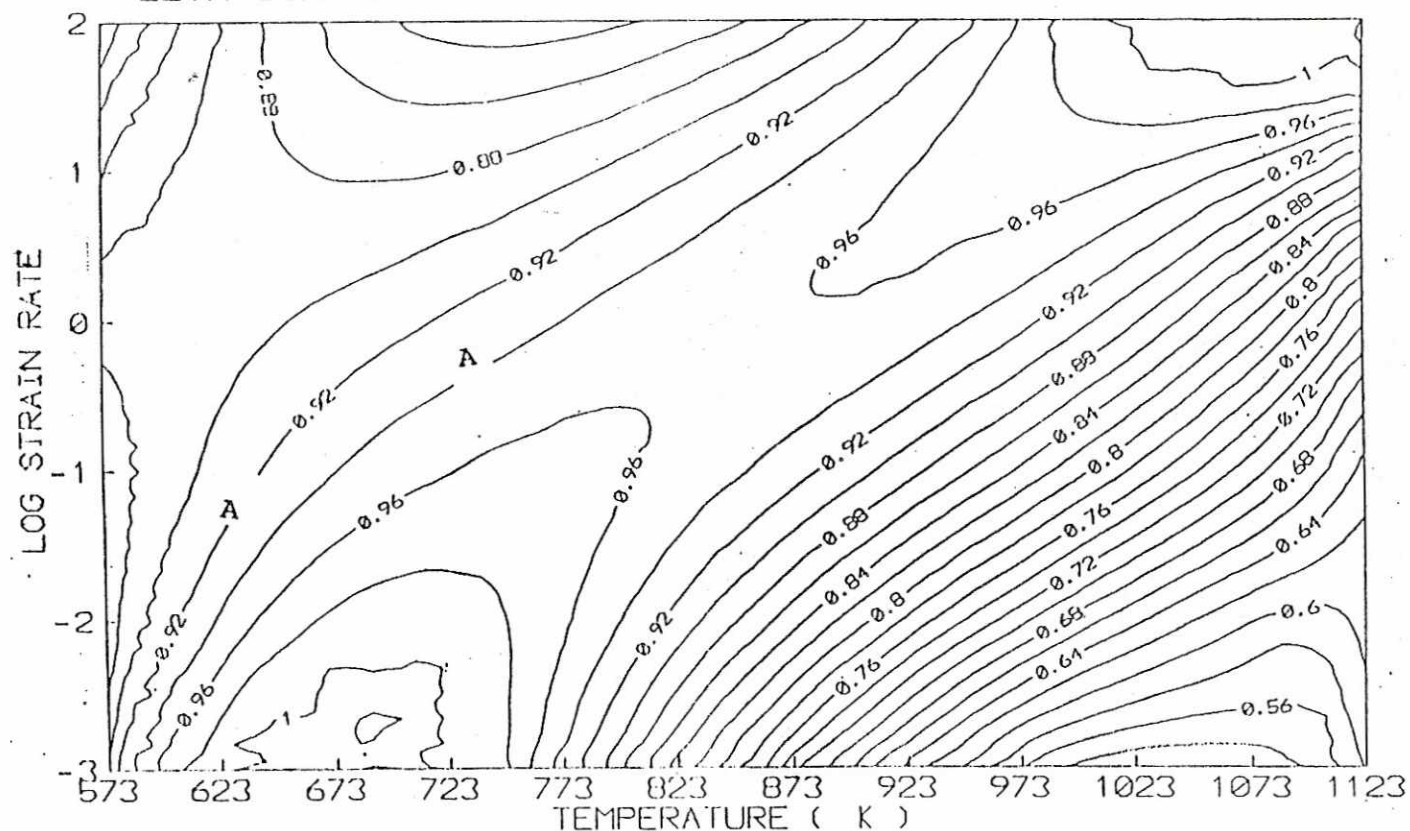

Fig. 7a. Two Dimensional Zeta Contour Map for Commercial Purity
Titanium at 0.1 Strain.

ZETA SURFACE PLOT FOR CP TITANIUM 0.1 STRAIN
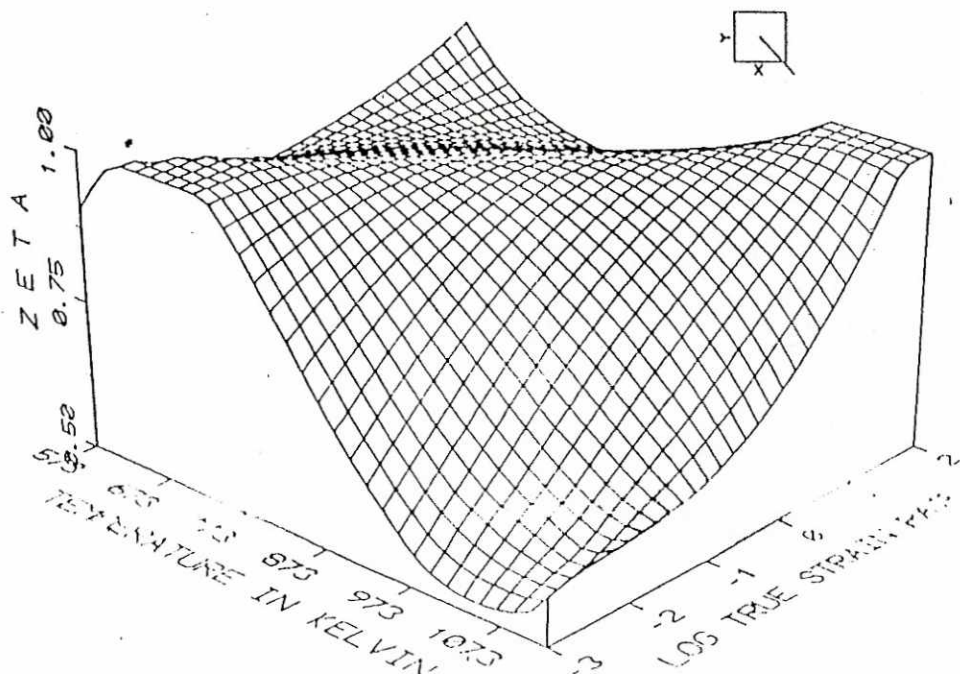
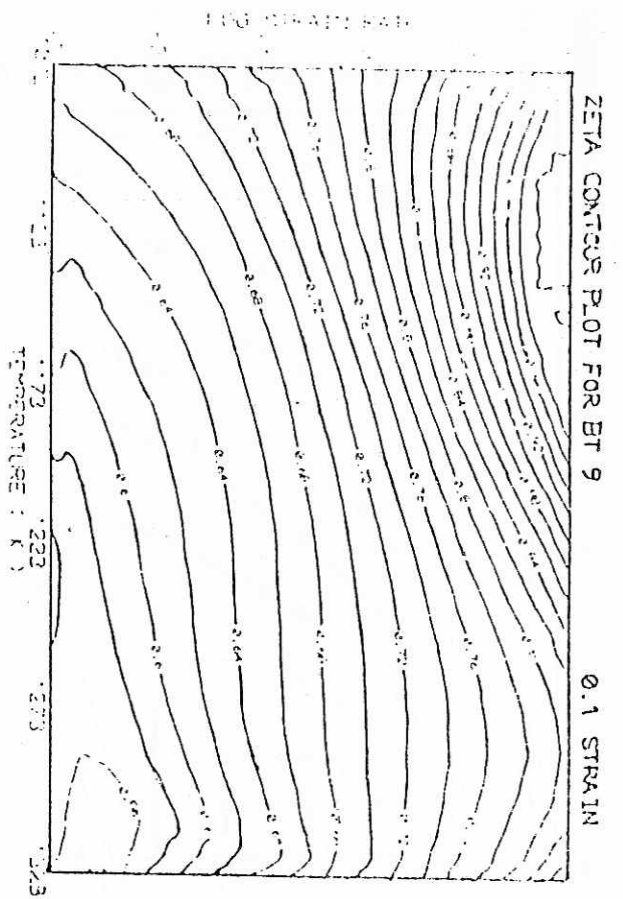

Fig. 7b. Three Dimensional Zeta Surface Map For Commercial Purity
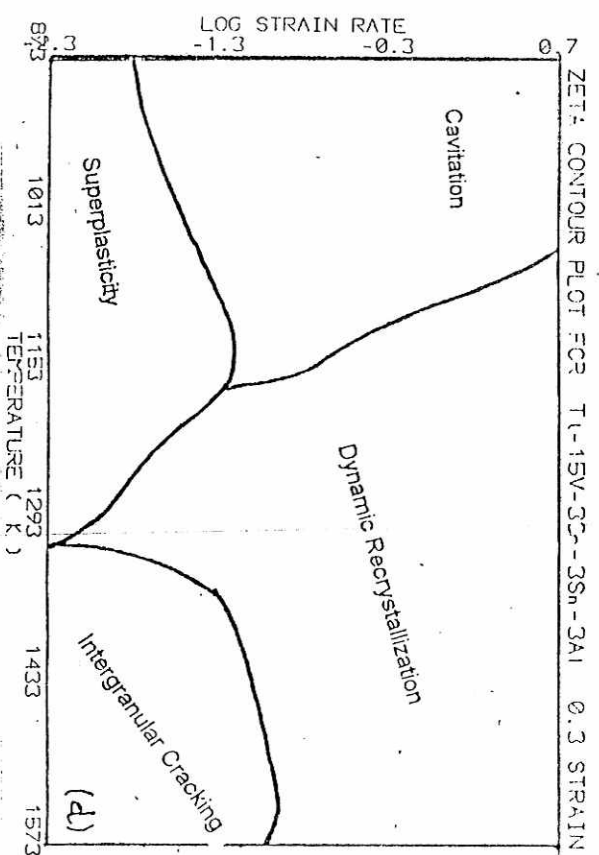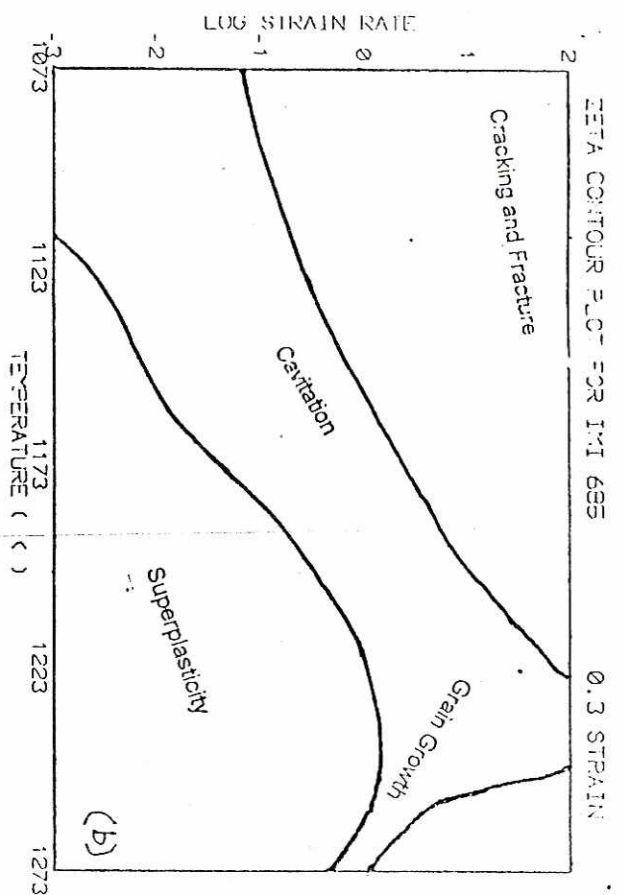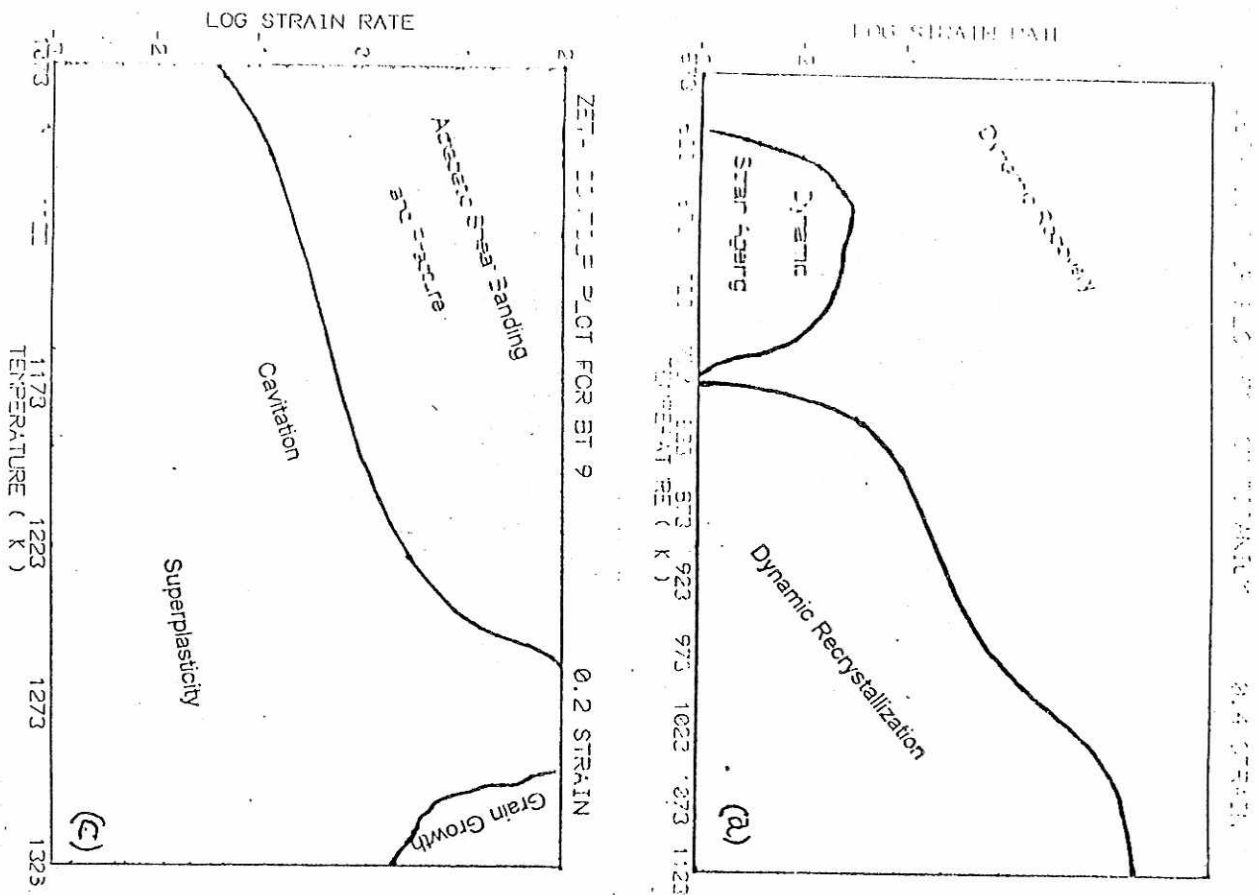Titanium At 0.1 Strain.

1·15

Fig 9. A series of ζ processing Maps for BT9 plotted at four different strains. Notice the shift of a lake bottom from 1323 K and 5 × 10⁻³ s⁻¹ at 0.1 strain to 1263 K and 3 × 10⁻³ s⁻¹ at 0.4 strain.

Fig 9. Summary of Processing Maps for a Range of Titanium Alloys.
(a) Cp-Ti
(b) Near α Alloy IMI 685
(c) (α + β) Alloy BT9
(d) Near β Alloy Ti6242

(a) LOG STRAIN RATE — TEMPERATURE (K) — Dynamic Recovery, Dynamic Shear Banding, Dynamic Recrystallization — 0.4 STRAIN

(b) ZETA CONTOUR PLOT FOR IMI 685 — LOG STRAIN RATE — TEMPERATURE (K) — Cracking and Fracture, Cavitation, Superplasticity, Grain Growth — 0.3 STRAIN

(c) ZETA CONTOUR PLOT FOR BT 9 — LOG STRAIN RATE — TEMPERATURE (K) — Adiabatic Shear Banding and Fracture, Cavitation, Superplasticity, Grain Growth — 0.2 STRAIN

(d) ZETA CONTOUR PLOT FOR Ti-15V-3Cr-3Sn-3Al — LOG STRAIN RATE — TEMPERATURE (K) — Cavitation, Superplasticity, Dynamic Recrystallization, Intergranular Cracking — 0.3 STRAIN

TABLE 1. THE RANGE OF ZETA AND THE MICROSCOPIC PHENOMENA

Magnitude of Zeta	Microscopic Phenomena
High 0.8 to 1.0	Cracking, Shear banding, Adiabatic shear banding, Grain growth, Dynamic strain ageing
Medium 0.7 to 0.8	Cavitation at Grain Boundaries, Dynamic recrystallization, Recovery
Low 0.5 to 0.7	Dynamic recovery, Dynamic recrystallization, Grain pinching, Texture softening, Superplasticity.
Very low <0.5	Superplasticity

TABLE 2: THE OPTIMUM HOT WORKING CONDITIONS FOR TITANIUM AND ITS ALLOYS

Alloy / feature	Cp-Titanium	BT5	IMI685	BT9	Ti-15333
1. Chemical Composition	Ti- Impurities	Ti-5Al-2.5Sn	Ti-6Al-0.5Mo-5Zr-0.1Si	Ti-6.5Al-1.65 Zr-3.3Mo-0.2Si	Ti-15V-3Cr-3Sn-3Al
2. Room temperature Phase composition	Alpha(h.c.p)	Alpha	Near Alpha	Alpha+Beta	Beta(b.c.c)
3. β transus °C	882	1040	1025	970	710
4. Testing conditions Temperature °C Strain rate (s^{-1})	300-850 10^{-3} to $10^{2} s^{-1}$	800-1050 10^{-3} to 10^{2}	800-1000 10^{-3} to 10^{2}	800-1050 10^{-3} to 10^{2}	600-1300 5×10^{-3} to 5×10^{0}
5. Predicted optimum working conditions (for 0.7 strain) and associated post deformation microstructure	740-1000°C and 10^{-3} to 10^{-1} s DRX of α Nearly equiaxed grains	1020-1040°C 10^{-3} to $10^{-1} s^{-1}$ DRX of α Nearly equiaxed grains	1000-1025°C 10^{-3} to $10^{-2} s^{-1}$ and 0.5 to 1×10^{2} s^{-1}; Superplastic flow; DRX Equiaxed grains	950°c and $5 \times 10^{-3} s^{-1}$ Grain pinching Microduplex fine grained structure	1150°C and $5 s^{-1}$ DRX of β: 600–1000^{0}X,10^{-2} s^{-1} Equiaxed grain structure ; DRX of beta; Superplasticity
6. Predicted worst working conditions and associated deformation microstructure	300°C and 10^{-2} s^{-1} Crack formation	800°C and 10^{2} s^{-1} Adiabatic shear banding and fracture	800°C and 10^{2} s^{-1} Adiabatic shear banding and fracture	800°C and 10^{2} s^{-1} Adiabatic shear banding and fracture	1150°C and 5×10-3s-1: 600-675°C 10^{-1}-5×10^{0}s^{-1} Grain Growth and Cracking
7. Industrial Practice or Observations	Worked at 870°C	Difficult work below 1020°C	Normally beta forged	Normally beta forged + alpha forged at 950°C	Not Known